Regular Paper (revised version to Journal of Biochemistry)

Mitochondrial nucleoid morphology and respiratory function are altered in Drp1-deficient HeLa cells

Azusa Ota[1,2], Takaya Ishihara[1,2], and Naotada Ishihara[1,2,*]

[1]Department of Biological Sciences, Graduate School of Science, Osaka University, 1-1 Machikaneyama-machi, Toyonaka, Osaka 560-0043, Japan

[2]Department of Protein Biochemistry, Institute of Life Science, Kurume University, 67 Asahi-machi, Kurume, Fukuoka 830-0011, Japan

[*]Corresponding author:

Department of Biological Science, Graduate school of Science, Osaka University

1-1 Machikaneyama-machi, Toyonaka, Osaka 560-0043, Japan

Tel.: +81-6-6850-6706; E-mail: naotada@bio.sci.osaka-u.ac.jp

Summary

Mitochondria are dynamic organelles that frequently divide and fuse with each other. The dynamin-related GTPase protein Drp1 has a key role in mitochondrial fission. To analyze the physiological roles of Drp1 in cultured human cells, we analyzed Drp1-deficient HeLa cells established by genome editing using CRISPR/Cas9. Under fluorescent microscopy, not only mitochondria were elongated but their DNA (mtDNA) nucleoids were extremely enlarged in bulb-like mitochondrial structures (“mito-bulbs”) in the Drp1-deficient HeLa cells. We further found that respiratory activity, as measured by oxygen consumption rates, was severely repressed in Drp1-deficient HeLa cells and that this was reversible by the co-repression of mitochondrial fusion factors. Although mtDNA copy number was not affected, several respiratory subunits were repressed in Drp1-deficient HeLa cells. These results suggest that mitochondrial fission is required for the maintenance of active respiratory activity and the morphology of mtDNA nucleoids in human cells.

Keywords: mitochondria, mtDNA, respiratory complex, membrane dynamics, GTPase

Mitochondria are dynamic organelles with a morphology regulated by a balance between fission and fusion (*1*). Drp1 is a dynamin-related GTPase protein that regulates mitochondrial fission. Drp1 is mainly localized in the cytoplasm and it is targeted to mitochondrial fission sites via mitochondrial surface receptor proteins, such as Mff, MiD49, and MiD51, to mediate mitochondrial fission. Two mitofusin proteins, Mfn1 and Mfn2, and Opa1 are localized to the mitochondrial outer and inner membrane, respectively, and regulate their fusion. The dynamic fusion and fission features of mitochondria are considered to be important not only for the maintenance of mitochondrial function but also for various cellular processes such as signaling, metabolism, and aging. Mfn2 and Opa1 have been identified as causal factors of the neurodegenerative disorders Charcot-Marie-Tooth neuropathy type 2a and dominant optic atrophy type 1, respectively (*2, 3, 4*), suggesting that mitochondrial fusion is essential for neuronal function. Defective mitochondrial fusion causes respiratory dysfunction in knockout (KO) mice and in RNA interference (RNAi) knock-down repressing these mitochondrial fusion factors in cultured mammalian cells such as mouse embryonic fibroblasts (MEFs) and HeLa cells (*5, 6, 7*). Yeast mutant strains defective in Fzo1 (yeast homolog of Mfn) or Mgm1 (yeast homolog of Opa1) also have impaired respiration (*8, 9*). Respiratory dysfunction was repressed by further inhibition of mitochondrial fission factors, suggesting that a balance between fusion and fission is required for the maintenance of respiratory function (*8, 9*).

Drp1 has a critical role in mammals *in vivo* because Drp1 KO mice are embryonic lethal (*10, 11*). Various tissue-specific Drp1 KO mice exhibit severe damage in each tissue, such as neurodegeneration in neuron-specific Drp1 KO mice (*10, 11*) and female infertility in oocyte-specific Drp1 KO mice (*12*). In contrast, Drp1 in mammals and the yeast homolog Dnm1 have been reported to be dispensable for cell growth in MEFs (*10*) and yeast cells (*13, 8, 9*), and these mitochondrial fission-deficient cells showed normal respiratory activity, supporting the notion that mitochondrial fission is not essential for the maintenance of respiratory activity, at least in some types of cells. However, several groups, including ours, have established and analyzed cardiomyocyte-specific Drp1 KO mice and found severe heart failure with respiratory dysfunction (*14, 15*). Several reports have suggested that defective mitochondrial fission leads to impaired

autophagic degradation of mitochondria (mitophagy) in cardiomyocytes, which should have a negative impact on mitochondrial quality control, resulting in respiratory deficiency (*15*). However, the detailed molecular mechanism underlying respiratory dysfunction by imbalanced mitochondrial fission and fusion is not well understood.

Mitochondria are believed to have originated from the endosymbiosis of bacteria and they have retained their own DNA, referred to as mitochondrial DNA (mtDNA) (*16, 17*). Under fluorescence microscopy using antibodies against nucleoid components, including DNA and TFAM, more than 100 dot-like structures known as mitochondrial nucleoids have been observed (*18, 19, 20*). We previously reported that mitochondrial fission tends to occur next to nucleoids and Drp1 RNAi causes the accumulation of mitochondrial nucleoids in bulb-like mitochondria ("mito-bulbs") with densely stacked cristae (*21*). We further found that mtDNA is highly accumulated in Drp1 KO mice cardiomyocytes in enlarged bulb-like mitochondria that exhibit active respiratory function. This suggests that the altered distribution of nucleoids might be related to respiratory dysfunction in the heart (*14*).

Drp1 has also been identified as a causal factor in humans with severe mitochondrial deficiency (*22*). To further elucidate the physiological roles of mitochondrial fission in human cells, we analyzed respiratory activity and nucleoid morphology in Drp1 KO HeLa cells and found that Drp1 is indispensable for the maintenance of respiratory activity and respiratory complexes, concomitant with nucleoid morphogenesis in HeLa cells.

Materials and methods

Reagents

SYBR Green I was purchased from Molecular Probes. MitoTracker Red CMXRos was purchased from Invitrogen. The following commercial antibodies were used: mouse monoclonal anti-DNA (AC-3010; Progen); mouse monoclonal anti-Drp1 (8/DLP1; BD Transduction); rabbit polyclonal anti-Tom20 (Santa Cruz Biotechnology); Total OXPHOS Rodent WB Antibody Cocktail (Abcam); rabbit polyclonal anti-VDAC1 (Abcam); mouse monoclonal anti-β-actin (AC-74; Sigma-Aldrich);

rabbit polyclonal anti-Mfn1 (Santa Cruz Biotechnology); mouse monoclonal anti-Mfn2 (4H8; Abnova); and Alexa Fluor 488-, 568-, or 660-labeled goat anti-mouse IgG_1 or IgM, or anti-rabbit IgG and HRP-conjugated anti-mouse or anti-rabbit IgG (Molecular Probes). Mammalian expression plasmid of 3×FLAG-rat Drp1 was described previously (*21*). Lipofectamine 2000 (Invitrogen) was used for plasmid transfection according to the manufacturer's protocol.

Cell culture, RNA interference by siRNA

HeLa cells were grown in Dulbecco's modified Eagle medium (DMEM; Wako Pure Chemical Industries) supplemented with 10% fetal bovine serum (FBS; Sigma-Aldrich). The establishment of Drp1 KO HeLa cells has been described previously (*23*). The target sequences of RNAi oligonucleotides (Silencer Select Pre-designed (Inventoried) siRNA) for Mfn1 and Mfn2 were purchased from ThermoFisher Scientific. We mixed and used s31220, s31219, and s31218 for Mfn1, and s19261, s19260, and s19262 for Mfn2. Luciferase siRNA and Negative control siRNA mixed and used as control were synthesized based on the following sequences: Luciferase siRNA (sense 5'-CGUACGCGGAAUACUUCGAdTdT-3'), Negative control siRNA (sense 5'-UACUAUUCGACACGCGAAGdTdT-3'). The siRNAs were introduced into HeLa cells by reverse transfection with RNAiMax (Invitrogen) according to the manufacturer's protocol. Briefly, the siRNAs, RNAiMax with Opti-MEM (Gibco) were mixed in a 96-well plate or a Seahorse XFp Cell Culture Miniplate and then HeLa Drp1 KO cells were seeded at a density of 2.5×10^3 cells/100 μL/well in the plate. After 24 h, the medium was changed. The cells were incubated for another 48h and performed in further investigations.

Live imaging and fluorescent microscopy

For live imaging, cells cultured on glass-bottomed dishes were stained with 0.1 μM MitoTracker Red for 15 min and 100,000-fold diluted SYBR Green I (*24*) for 5 min at 37°C, washed twice with growth medium, and changed to fresh growth medium containing 50 mM HEPES buffer (pH 7.4). After 30 min, the cells were observed under a BZ-X700/BZ-X710 microscope (Keyence).

Cell growth

Cell growth was measured using a CellTiter-Fluor Cell Viability Assay (Promega). 1.25×10^3 cells were seeded in a 96-well plate of culture medium for at least 6 h before measurement. The culture medium was exchanged with 100 μL/well measurement medium mixture (50 μL FluoroBrite DMEM (Gibco), 49.95 μL assay buffer, and 0.05 μL GF-AFC substrate). The plate was incubated at 37°C for 90 min. After incubation, the plate was measured using an Infinite F200 PRO plate reader (Tecan) (400 nm_{EX}/505 nm_{EM}).

Quantitative PCR and analysis of mtDNA copy number

DNA from HeLa cells was extracted using a QIAamp DNA Mini Kit (Qiagen) according to the manufacturer's instructions. A KAPA SYBR FAST qPCR Kit was used for quantitative PCR with an ABI StepOne plus (Applied Biosystems). To produce a standard curve, we used 0.5, 1, 2, 4, and 8 ng of untreated HeLa cell DNA for mtDNA amplification or 1, 2, 4, 8, and 16 ng of untreated HeLa cell DNA for nuclear gene amplification. The primer sets for the amplification of mtDNA (65 bp) and β2M coding nuclear DNA (95 bp) fragments were used as described previously (*25*).

Oxygen consumption rate

For measurements of respiration rates by a Clark electrode, 5.0×10^6 cells were washed with respiration buffer (30 mM HEPES, 75 mM sucrose, 20 mM glucose, 5 mM potassium phosphate buffer [pH 7.1], 40 mM KCl, 0.5 mM EDTA, and 3 mM $MgCl_2$). The pellet was suspended in respiration buffer I (50-fold diluted protease inhibitor cocktail tablet (Complete EDTA-free, Roche] and 1 mM phenylmethylsulfonyl fluoride (PMSF) in respiration buffer). An equal volume of respiration buffer I containing 0.01% digitonin was added to the cell suspension. The mixture was incubated for 5 min at room temperature. Permeabilization was stopped at 4°C by the addition of a 10-fold volume of respiration buffer II (0.3% bovine serum albumin and a 50-fold diluted protease inhibitor cocktail tablet (Complete EDTA-free] in respiration buffer. The permeabilized cells were

collected by swing-type centrifugation by 2500 rpm for 5 min at 4°C and resuspended in respiration buffer containing 50-fold diluted protease inhibitor cocktail tablet (Complete EDTA-free). Oxygen consumption was measured in whole cells at room temperature using an Oxytherm+ Clark-type electrode (Hansatech Instruments) in the presence of 1 mM ADP. Glutamate and malate were added at 5 mM each. Next, 10 mM succinate and 10 μM rotenone were added. Then 10 mM ascorbate, 400 μM TMPD, and 20 μM antimycin A were added. Finally, uncoupler DNP was added at 25 μM. After the recording, respiration was blocked with 0.75 mM KCN.

Oxygen consumption was measured at 37°C using a Seahorse XFp Analyzer (Agilent Technologies). The cells were seeded at a density of 2.0×10^4 cells/80 μL/well in 3 different wells of an XFp cell culture plate. The next day, the cell culture medium was removed from the plate, the cells were washed twice with fresh medium, and then cultured in pre-warmed Seahorse medium supplemented with 25 mM glucose, 1 mM pyruvate, 2 mM glutamine, and 1% FBS in a CO_2-free incubator at 37°C for 1 h. Measurements of endogenous respiration were performed using 1 μM oligomycin, 1 μM carbonyl cyanide-4-(trifluoromethoxy)phenylhydrazone (FCCP), and 0.5 μM rotenone/antimycin A. All oxygen consumption rates and bioenergetic parameters were determined as indicated in Seahorse XF Cell Mito Stress Test Report Generator from Wave Software. The results were normalized to μg of protein/well quantified after each Seahorse run, using a Pierce BCA Protein Assay Kit (Thermo Fisher Scientific) according to the manufacturer's instructions.

Immunofluorescence staining of fixed cells

Cells grown on coverslips were fixed for 15 min with 4% paraformaldehyde, washed twice with PBS, and permeabilized for 5 min with 0.2% Triton X-100 in PBS. After three washes with PBS, cells were blocked for 1h with 5% skim milk in PBS, then incubated with primary antibodies for 1 h at room temperature. After four washes with PBS, cells were incubated with secondary antibodies for 1 h at room temperature. After four washes with PBS, the coverslips were mounted (SlowFade Gold antifade reagent; Molecular Probes). Samples were observed under an Olympus IX81 fluorescence microscope. Images were analyzed using Metamorph software (Molecular Devices).

Immunoblotting

Proteins were separated by polyacrylamide gel electrophoresis and transferred to polyvinylidene fluoride (PVDF) membranes. The membranes were blocked with 5% skim milk in tris-buffered saline with Tween 20 and incubated with the indicated primary antibodies followed by mouse or rabbit horseradish peroxidase-conjugated secondary antibodies. Blots were detected with ECL (GE Healthcare).

Results and discussion

Mitochondrial and nucleoid morphology are altered in Drp1 KO HeLa cells

Nucleoids become highly clustered in elongated bulb-like mitochondria in Drp1 RNAi HeLa cells (*21*). Here, we investigated the morphology of mitochondria and their nucleoids in Drp1 KO HeLa cells, which we established previously by genome editing (*23*). As reported previously, Drp1 KO HeLa cells showed elongated mitochondria with many mito-bulb structures ("Drp1 KO HeLa," Fig 1A), compared with control wild-type (WT) HeLa cells ("WT HeLa," Fig 1A). We further found that the number of nucleoids was decreased (Fig 1A and B), and the each of nucleoids was enlarged (Fig 1A and C). These phenotypes were basically similar to those seen in Drp1 RNAi cells, although Drp1 KO in HeLa cells induced a more severe phenotype, forming greatly enlarged nucleoids compared with Drp1 RNAi HeLa cells (*21*) and Drp1 KO MEFs (*10*). These results suggest that the mitochondrial fission factor Drp1 regulates nucleoid distribution in HeLa cells.

Oxygen consumption is severely repressed in Drp1 KO HeLa cells but mtDNA copy number is not affected

Next, we measured mtDNA copy number because it should be decreased in mitochondrial fusion-deficient cells, leading to respiratory dysfunction (*7*). When we measured mtDNA using real-time quantitative polymerase chain reaction (PCR), mtDNA copy number was similar between

Drp1 KO HeLa cells and WT HeLa cells (Fig 2A), suggesting that mitochondrial fission is dispensable for the maintenance of mtDNA in HeLa cells. We then measured the growth rate of Drp1 KO cells and found that Drp1 KO HeLa cells grew more slowly than WT HeLa cells (Fig 2B), suggesting that Drp1 is required for cellular function.

Next, we measured the respiratory activity of Drp1 KO HeLa cells. First, HeLa cells were permeabilized by treatment with digitonin and oxygen concentration was measured using a Clark electrode. To analyze the activity of each respiratory complex, we measured oxygen concentration in the presence of ADP after sequentially adding various respiratory substrates: glutamate and malate to measure complex I; succinate to measure complex II; and ascorbate and N, N, N′ , N′ -tetramethyl-p-diaminobenzene perchlorate (TMPD) for complex IV; then dinitrophenol (DNP) was added to measure maximum respiration. From these analyses, we found that respiratory activity was severely affected in Drp1 KO HeLa cells in all conditions examined (Fig 2C), suggesting that complete blockage of Drp1 by the genome editing impaired respiratory activity in HeLa cells.

Similar results were also obtained by measurement of oxygen consumption in living cultured HeLa cells using a Seahorse analyzer XFp (Fig 3A-C), showing that basal (Fig 3A and B) and maximal (Fig 3A and C) activities were severely repressed in Drp1 KO HeLa cells. We also found that mtDNA nucleoids clustered and respiratory dysfunction were partly but clearly rescued by re-introduction of FLAG-tagged Drp1 to the Drp1 KO HeLa cells (Fig 3D-F), suggesting that these effects are specific for the Drp1 KO, not by an off-target effect. These data further supports the conclusion that Drp1-dependent mitochondrial fission is essential for the maintenance of respiratory activity (model, Fig 7).

Respiratory subunits are decreased in Drp1 KO HeLa cells

mtDNA encodes 13 respiratory subunits and produces RNA for mito-ribosomes and transfer RNAs. These 13 proteins are subunits of complexes I, III, and IV and Fo-ATPase, while all of the complex II subunits are encoded by the nuclear genome. Here, we examined the protein levels of respiratory subunits by immunoblotting and found that respiratory chain subunits, including NDUFB8 in

complex I, UQCRC2 in complex III, and COX I in complex IV, were significantly decreased in Drp1 KO HeLa cells (Fig 4 A and B), suggesting that Drp1 is required for the expression and/or stabilization of mtDNA-encoded respiratory subunits and thus leads to respiratory dysfunction (Figs 2C and 3). In contrast, the protein level of the complex II subunit SDHB was only weakly repressed compared with the other respiratory subunits, suggesting that the expression of mtDNA should be impaired in Drp1 KO HeLa cells. This might be caused by the deformed nucleoid morphology in these cells (Fig 1 and model, Fig 7), although the detailed molecular mechanism remains to be analyzed.

Mitochondrial fusion and fission balance is critical for nucleoid morphology and cell growth

Mitochondrial morphology is regulated by a balance between fusion and fission. Furthermore, defective respiratory function in mitochondrial fusion-deficient cells can be rescued by the co-repression of mitochondrial fission; for example, the respiratory dysfunction observed in the fzo1 mutant yeast strain can be recovered by introducing a further mutation into dnm1 (*8*). To analyze the roles of the balance of mitochondrial fusion and fission in the morphology of mitochondria and nucleoids as well as in respiratory function, both of two Mfn isoforms (Mfn1 and Mfn2) were repressed in Drp1 KO HeLa cells by RNAi (Fig 5C). We found that the elongated mitochondria with mito-bulb structures were resolved to form a fragmented mitochondrial network (Fig 5A, red). When mtDNA was stained using SYBR Green I, the enlarged nucleoids were found to have disappeared and formed many small nucleoids, as observed in WT HeLa cells (Fig 5A, green). By the RNAi repression of Mfn1 and Mfn2, the number of nucleoids was 4.65 fold increased (p=0.0116), and the average size of nucleoids was 0.50 fold reduced (p=0.0215), compared with those of Drp1 KO cells. We also found that RNAi of Mfn1 and Mfn2 partly suppressed growth retardation of Drp1 KO HeLa cells (Fig 5B). When we analyzed respiratory activity using a Seahorse flux analyzer, respiratory activity was rescued by RNAi of Mfns in Drp1 KO HeLa cells (Fig 6A-C). As expected, RNAi of Mfn1 and Mfn2 repressed maximal respiratory activity in WT cells (Fig 6D and E), inconsistent with the increased respiration in Drp1 KO cells (Fig 6B and C), suggesting that the fusion-fission balance

is crucial for the maintenance of mitochondrial activity. Thus, the enlarged nucleoids and respiratory dysfunction induced by Drp1 KO in HeLa cells could be rescued by repressing mitochondrial fusion factors, resolving the clustered nucleoids and rescuing oxygen consumption (model, Fig 7).

In conclusion, defective mitochondrial fission led to the accumulation and clustering of nucleoids to form a smaller number of enlarged nucleoids, but they were reversible structures regulated by fusion and fission. Respiratory function was also regulated by Drp1-dependent mitochondrial fission. However, it remains unclear whether and how nucleoid clustering affects respiratory activity and respiratory complex formation. These Drp1 KO phenotypes should be altered according to the differentiation state of cells because respiratory activity was more effective in the cardiomyocytes compared with MEFs. It might also be possible that species-specific characteristics have a role in these processes, in which human cells might be more sensitive to the imbalance of mitochondrial fusion and fission than mice cells. The tissue-specific function of mitochondrial fission should be a candidate therapeutic target in differentiated tissues, although further analysis is needed to determine its physiological roles *in vivo*.

Funding

This work was supported by the Japanese Society for the Promotion of Science KAKENHI (NI, Grant Number 17H03677), by AMED-CREST (NI; under Grant Number JP19gm1110006, 19gm0810009) MEXT-Supported Program for the Strategic Research Foundation at Private Universities (NI).

REFERENCES

1. Ishihara T, Kohno H, Ishihara N. (2015) Physiological roles of mitochondrial fission in cultured cells and mouse development. Ann N Y Acad Sci 1350: 77-81.

2. Delettre C, Lenaers G, Griffoin JM, Gigarel N, Lorenzo C, Belenguer P, Pelloquin L, Grosgeorge J, Turc-Carel C, Perret E, Astarie-Dequeker C, Lasquellec L, Arnaud B, Ducommun B, Kaplan J, Hamel CP. (2000) Nuclear gene OPA1, encoding a mitochondrial dynamin-related protein, is mutated in dominant optic atrophy. Nat Genet 26(2): 207-210.

3. Alexander C, Votruba M, Pesch UE, Thiselton DL, Mayer S, Moore A, Rodriguez M, Kellner U, Leo-Kottler B, Auburger G, Bhattacharya SS, Wissinger B. (2000) OPA1, encoding a dynamin-related GTPase, is mutated in autosomal dominant optic atrophy linked to chromosome 3q28. Nat Genet 26(2): 211-215.

4. Zuchner S, Mersiyanova IV, Muglia M, Bissar-Tadmouri N, Rochelle J, Dadali EL, Zappia M, Nelis E, Patitucci A, Senderek J, Parman Y, Evgrafov O, Jonghe PD, Takahashi Y, Tsuji S, Pericak-Vance MA, Quattrone A, Battaloglu E, Polyakov AV, Timmerman V, Schroder JM, Vance JM. (2004) Mutations in the mitochondrial GTPase mitofusin 2 cause Charcot-Marie-Tooth neuropathy type 2A. Nat Genet 36(5): 449-451.

5. Chen H, Chomyn A, Chan DC. (2005) Disruption of fusion results in mitochondrial heterogeneity and dysfunction. J Biol Chem 280(28): 26185-26192.

6. Chen H, McCaffery JM, Chan DC. (2007) Mitochondrial fusion protects against neurodegeneration in the cerebellum. Cell 130(3): 548-562.

7. Chen H, Vermulst M, Wang YE, Chomyn A, Prolla TA, McCaffery JM, Chan DC. (2010) Mitochondrial fusion is required for mtDNA stability in skeletal muscle and tolerance of mtDNA mutations. Cell 141(2): 280-289.

8. Jensen RE, Hobbs AE, Cerveny KL, Sesaki H. (2000) Yeast mitochondrial dynamics: fusion, division, segregation, and shape. Microsc Res Tech 51(6): 573-583.

9. Sesaki H, Southard SM, Yaffe MP, Jensen RE. (2003) Mgm1p, a dynamin-related GTPase, is essential for fusion of the mitochondrial outer membrane. Mol Biol Cell 14(6): 2342-2356.

10. Ishihara N, Nomura M, Jofuku A, Kato H, Suzuki SO, Masuda K, Otera H, Nakanishi Y, Nonaka I, Goto Y, Taguchi N, Morinaga H, Maeda M, Takayanagi R, Yokota S, Mihara K. (2009) Mitochondrial fission factor Drp1 is essential for embryonic development and synapse formation in mice. Nat Cell Biol 11(8): 958-966.

11. Wakabayashi J, Zhang Z, Wakabayashi N, Tamura Y, Fukaya M, Kensler TW, Iijima M, Sesaki H. (2009) The dynamin-related GTPase Drp1 is required for embryonic and brain development in mice. J Cell Biol 186(6): 805-816.

12. Udagawa O, Ishihara T, Maeda M, Matsunaga Y, Tsukamoto S, Kawano N, Miyado K, Shitara H, Yokota S, Nomura M, Mihara K, Mizushima N, Ishihara N. (2014) Mitochondrial fission factor

Drp1 maintains oocyte quality via dynamic rearrangement of multiple organelles. Curr Biol 24(20): 2451-2458.

13. Otsuga D, Keegan BR, Brisch E, Thatcher JW, Hermann GJ, Bleazard W, Shaw JM. (1998) The dynamin-related GTPase, Dnm1p, controls mitochondrial morphology in yeast. J Cell Biol 143(2): 333-349.

14. Ishihara T, Ban-Ishihara R, Maeda M, Matsunaga Y, Ichimura A, Kyogoku S, Aoki H, Katada S, Nakada K, Nomura M, Mizushima N, Mihara K, Ishihara N. (2015) Dynamics of mitochondrial DNA nucleoids regulated by mitochondrial fission is essential for maintenance of homogeneously active mitochondria during neonatal heart development. Mol Cell Biol 35(1): 211-223.

15. Ikeda Y, Shirakabe A, Maejima Y, Zhai P, Sciarretta S, Toli J, Nomura M, Mihara K, Egashira K, Ohishi M, Abdellatif M, Sadoshima J. (2015) Endogenous Drp1 mediates mitochondrial autophagy and protects the heart against energy stress. Circ Res 116(2): 264-278.

16. Lang BF, Burger G, O'Kelly CJ, Cedergren R, Golding GB, Lemieux C, Sankoff D, Turmel M, Gray MW. (1997) An ancestral mitochondrial DNA resembling a eubacterial genome in miniature. Nature 387(6632): 493-497.

17. Kuroiwa T. (2010) Mechanisms of organelle division and inheritance and their implications regarding the origin of eukaryotic cells. Proc Jpn Acad Ser B Phys Biol Sci 86(5): 455-471.

18. Garrido N, Griparic L, Jokitalo E, Wartiovaara J, van der Bliek AM, Spelbrink JN. (2003)

Composition and dynamics of human mitochondrial nucleoids. Mol Biol Cell 14(4): 1583-1596.

19. Legros F, Malka F, Frachon P, Lombes A, Rojo M. (2004) Organization and dynamics of human mitochondrial DNA. J Cell Sci 117(Pt 13): 2653-2662.

20. Iborra FJ, Kimura H, Cook PR. (2004) The functional organization of mitochondrial genomes in human cells. BMC Biol 2:9.

21. Ban-Ishihara R, Ishihara T, Sasaki N, Mihara K, Ishihara N. (2013) Dynamics of nucleoid structure regulated by mitochondrial fission contributes to cristae reformation and release of cytochrome c. Proc Natl Acad Sci U S A 110(29): 11863-11868.

22. Whitley BN, Lam C, Cui H, Haude K, Bai R, Escobar L, Hamilton A, Brady L, Tarnopolsky MA, Dengle L, Picker J, Lincoln S, Lackner LL, Glass IA, Hoppins S. (2018) Aberrant Drp1-mediated mitochondrial division presents in humans with variable outcomes. Hum Mol Genet 27(21): 3710-3719.

23. Saita S, Ishihara T, Maeda M, Iemura S, Natsume T, Mihara K, Ishihara N. (2016) Distinct types of protease systems are involved in homeostasis regulation of mitochondrial morphology via balanced fusion and fission. Genes to Cells 21(5): 408-424.

24. Ozawa S, Sasaki N. (2009) Visualization of mitochondrial nucleoids in living human cells using SYBR Green I. Cytologia (Tokyo) 74:366.

25. Malik AN, Shahni R, Rodriguez-de-Ledesma A, Laftah A, Cunningham P. (2011) Mitochondrial

1 DNA as a non-invasive biomarker: accurate quantification using real time quantitative PCR without

2 co-amplification of pseudogenes and dilution bias. Biochem Biophys Res Commun 412(1): 1-7.

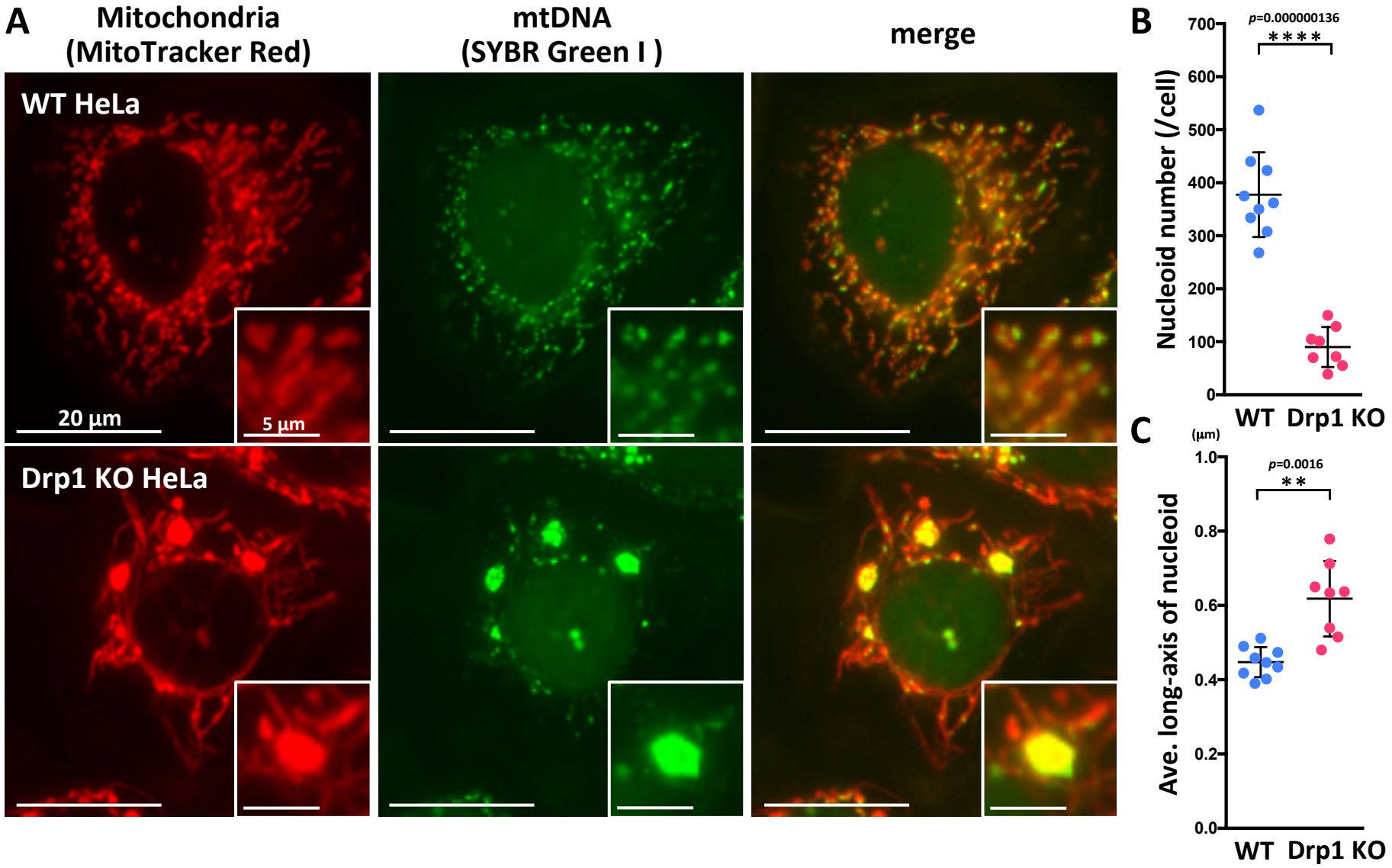

Figure 1. Mitochondrial and nucleoid morphology in Drp1 KO HeLa cells.
Wild-type (WT) and Drp1 KO HeLa cells were stained with MitoTracker Red (mitochondria) for 15 min and with SYBR Green I (mitochondrial DNA nucleoids) for 5 min. The cells were observed by fluorescence microscopy (A), then the number (B) and the size of nucleoids (C), measuring a length of the long-axis of nucleoid, were measured. Scale bar: 20 µm in the large panels and 5 µm in the insets.

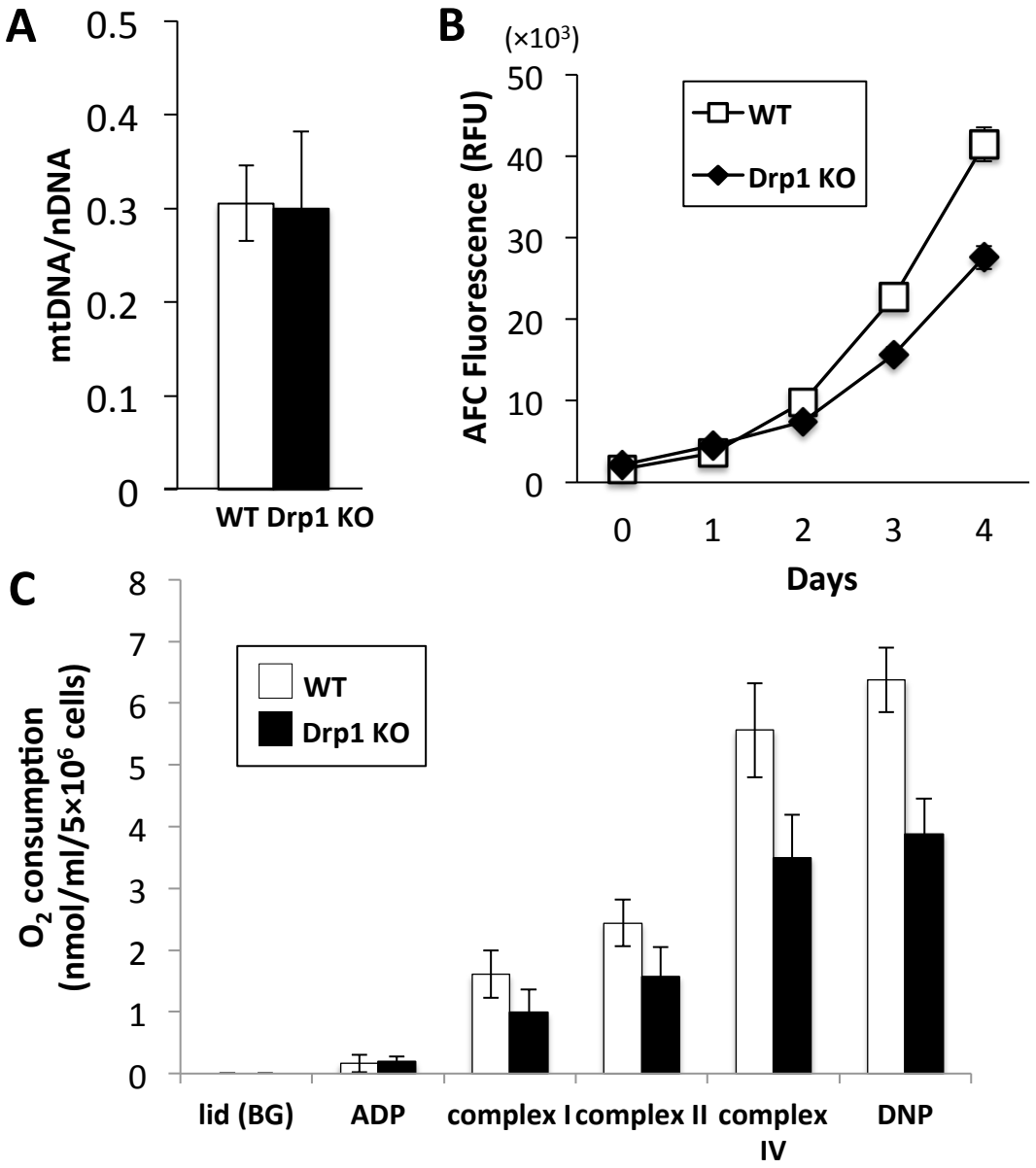

Figure 2. MtDNA copy number (A), growth rate (B), and oxygen consumption measured by a Clark-type electrode (C) of Drp1 KO HeLa cells. (A) The mtDNA content of WT and Drp1 KO HeLa cells was quantified by quantitative PCR. The relative amount of mtDNA (nt: 317–381, 65 bp) per nuclear gene (β2M, 95 bp) is shown. (B) Cell growth rates of WT and Drp1 KO HeLa cells. (C) Oxygen consumption rates of permeabilized WT and Drp1 KO HeLa cells were measured using a Clark electrode in the presence of the indicated respiratory substrates.

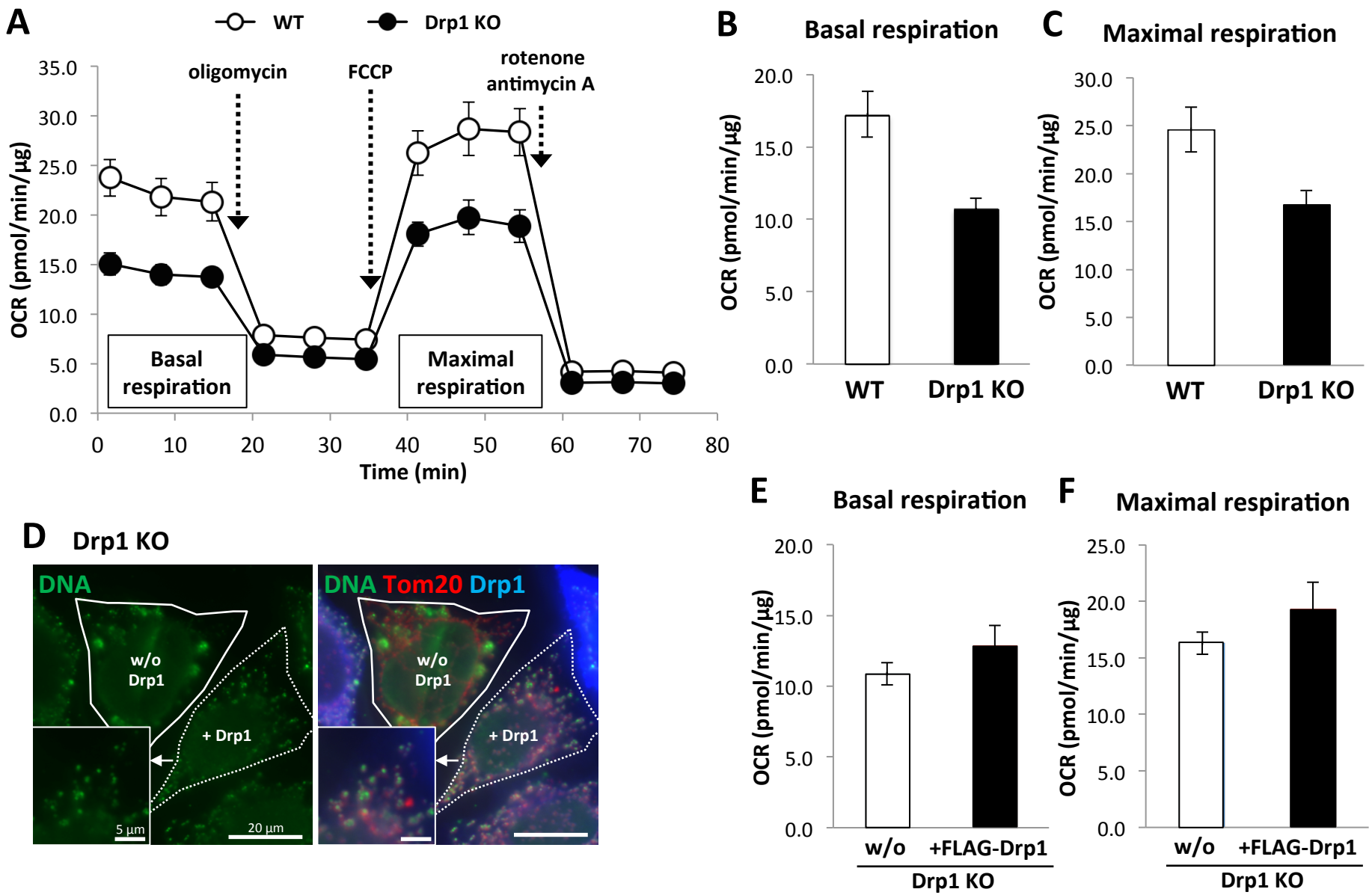

Figure 3. Oxygen consumption of Drp1 KO HeLa cells measured using a Seahorse flux analyzer.
(A-C) Oxygen consumption rates of WT and Drp1 KO HeLa cells were measured using a Seahorse analyzer XFp. From the recording of oxygen consumption rates (A), the basal respiration (B) and maximal respiration (C) were calculated. (D-F) FLAG-tagged Drp1 was exogenously expressed to Drp1 KO HeLa cells for 24 h, and mtDNA (anti-DNA: green), mitochondria (anti-Tom20: red), and Drp1 (anti-Drp1: blue) were analyzed by immunofluorescence microscopy (D). The basal respiration (E) and maximal respiration (F) of respiratory activities were calculated as above.

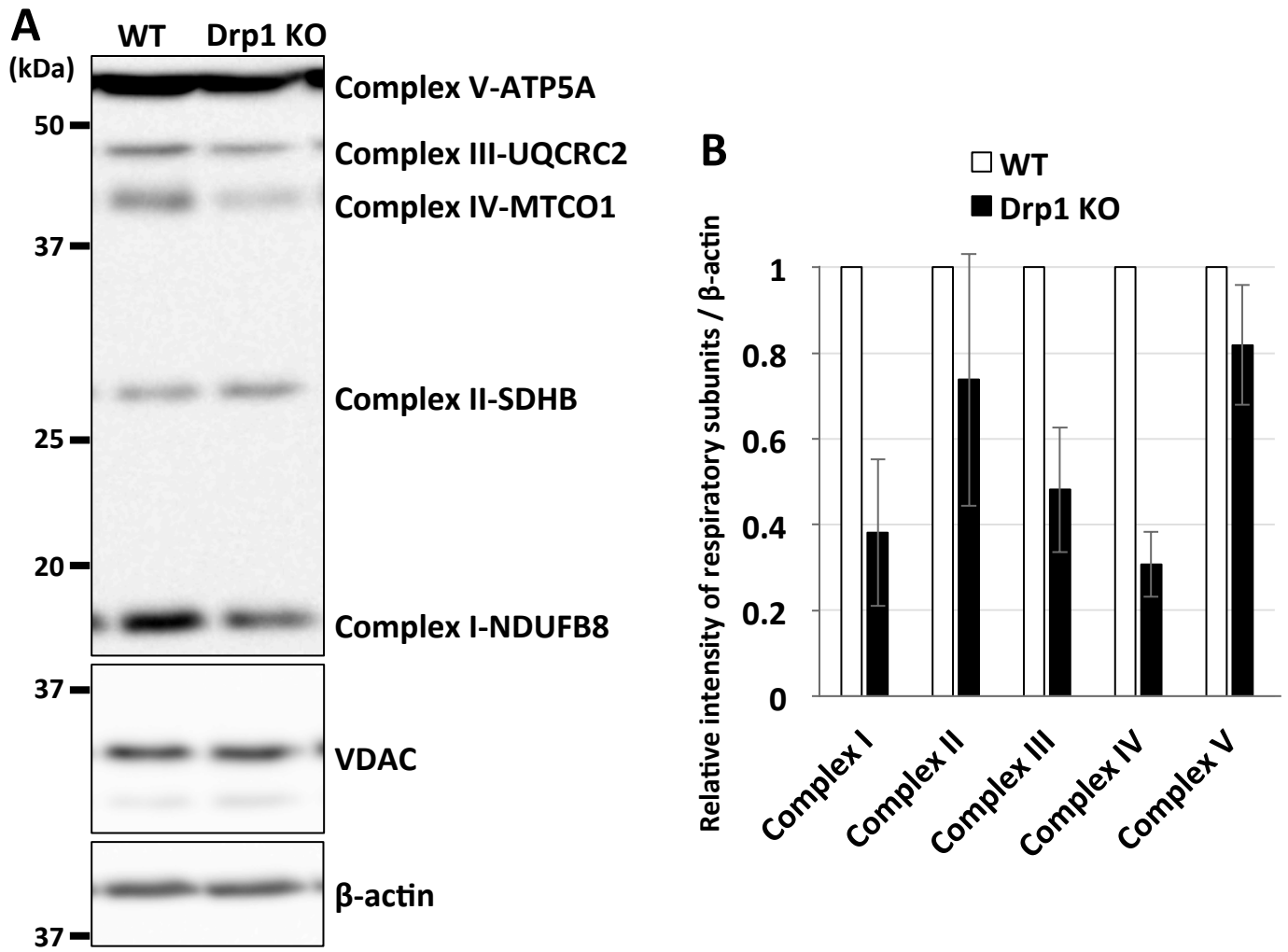

Figure 4. Protein levels of respiratory subunits in Drp1 KO HeLa cells.
(A) Protein levels in WT and Drp1 KO HeLa cells were determined by immunoblotting using the indicated antibodies. (B) Quantification of respiratory subunits from four independent immunoblot experiments as (A). The *p*-values from Welch's t-test are 0.0054 (complex I), 0.17 (complex II), 0.0057 (complex III), 0.00036 (complex IV), and 0.080 (complex V).

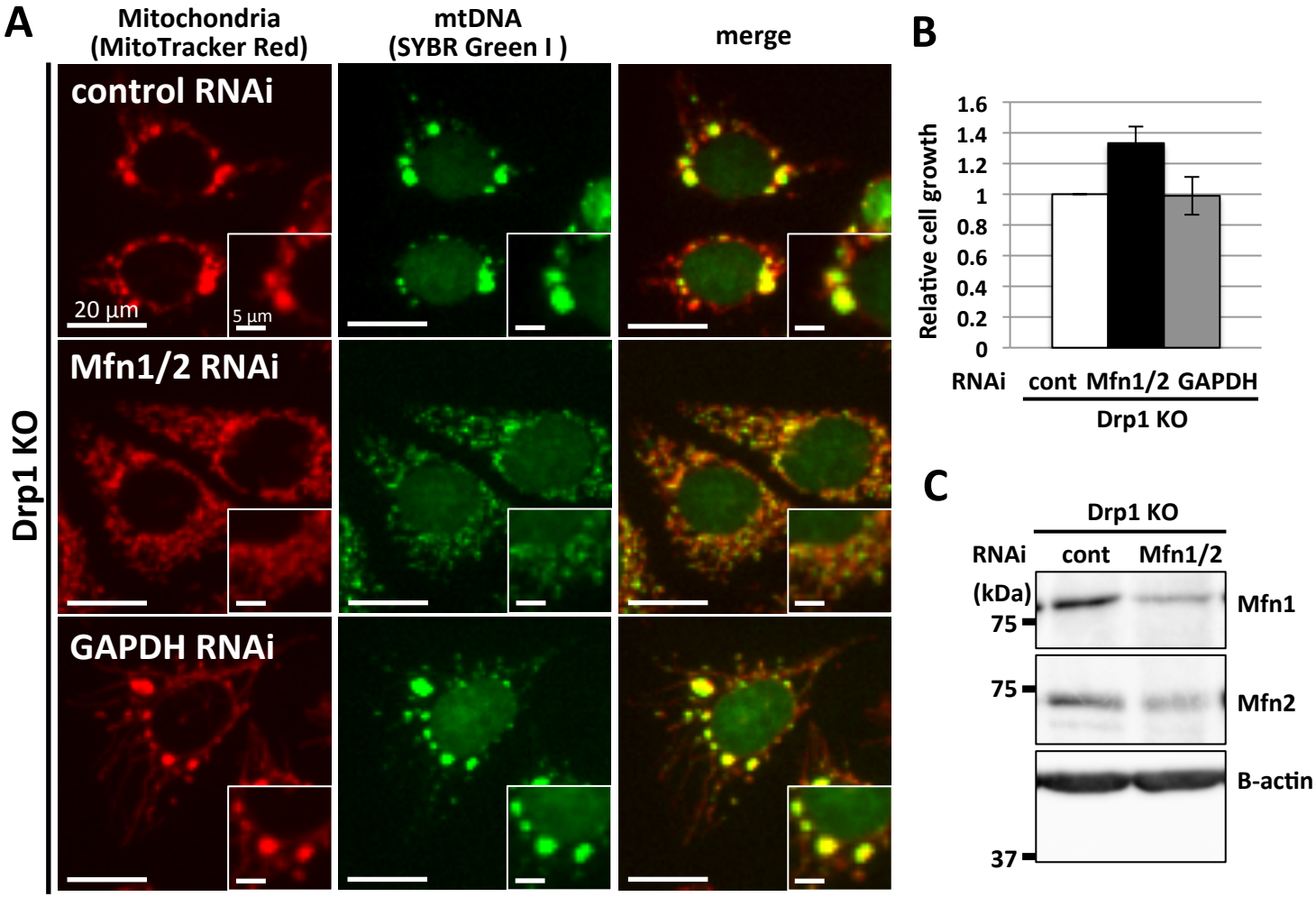

Figure 5. Mitochondrial fusion and fission balance is critical for nucleoid morphology and cell growth.
Rescue experiments on mito-bulb formation with nucleoid clustering. Drp1 KO HeLa cells were treated with siRNA targeting mitofusin proteins Mfn1 and Mfn2 or control for 72 h. (A) Images of nucleoids and mitochondria by fluorescence staining of each cells. Scale bar: 20 µm in the large panels and 5 µm in the insets. (B) Cell growth rates of Drp1 KO HeLa cells treated with siRNA targeting Mfn1 and Mfn2 for 72 h. (C) Immunoblotting of Mfn proteins after the RNAi treatment.

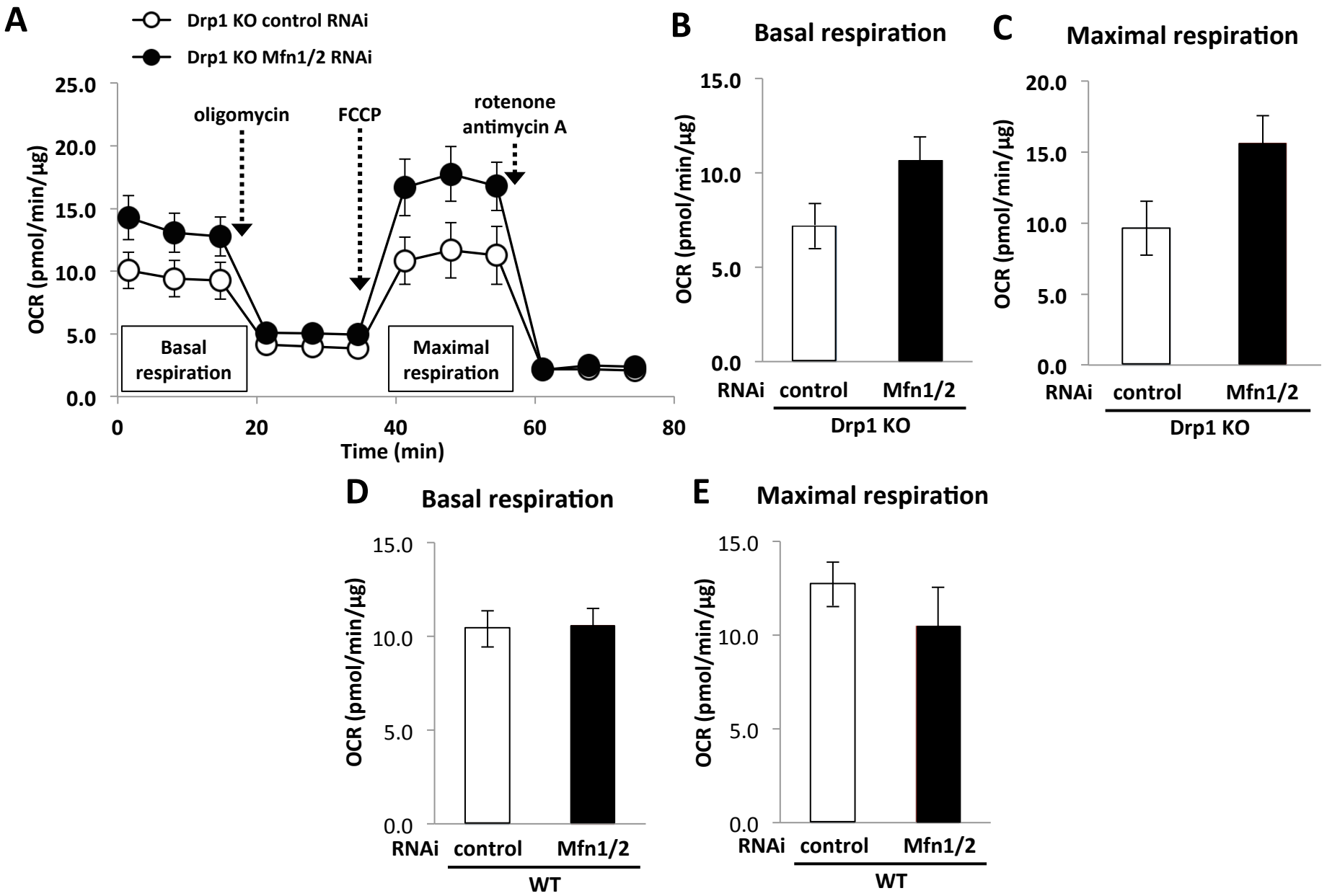

Figure 6. Balanced mitochondrial fusion and fission is critical for respiratory activity.
Drp1 KO HeLa cells (A-C) and WT HeLa cells (D and E) were treated with siRNA targeting Mfn1 and Mfn2 or control for 72 h. Oxygen consumption rates were measured using a Seahorse analyzer XFp. From the recording of oxygen consumption rates (A), the basal respiration (B) and maximal respiration (C) were calculated. The basal respiration (D) and maximal respiration (E) of respiratory activities were calculated as above.

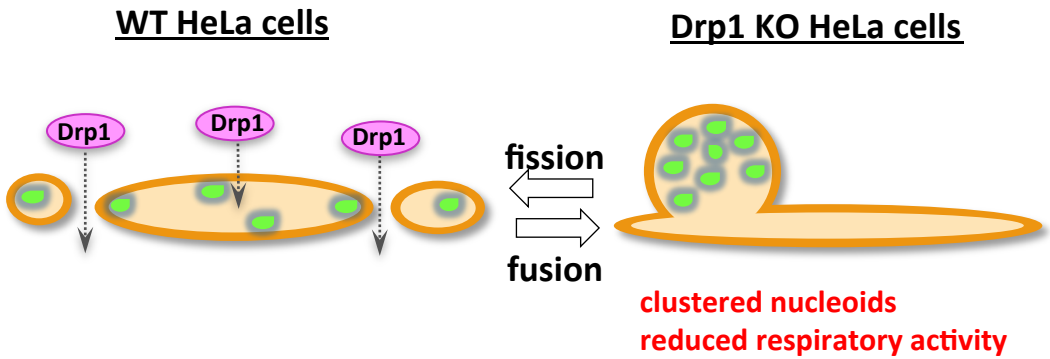

Figure 7. Schematic model of nucleoid structure and respiration regulated by mitochondrial fission in HeLa cells. See details in text.